Research Journal of Applied Sciences 11 (11): 1391-1398, 2016
ISSN: 1815-932X
© Medwell Journals, 2016

Interpretation of Gravity and Magnetic Data Using Continuous Wavelet Transforms

[1]Arash Amirian, [1]Seyed Ali Akbar Motamedi and [2]Javad Hamzelo
[1]Faculty of Science, Razi University, Kermanshah, Iran
[2]Faculty of Engineering, University of Bologna, Bologna, Italy

Abstract: Continuous wavelet transform is used to analyze potential fields (magnetic, gravity, VLF, SP…) as well as locating their related sources. It is possible to determine the location of a source edge by wavelet space which is obtained by Poisson wavelets. When the source is perfectly homogeneous, the degree of homogeneity is also determined. In addition, more source homogeneity results in higher accuracy of edge detection. The effect of noise is also investigated. The wavelet transform removes high frequency noises automatically as it acts as an upward continuation operator.

Key words: Wavelet transforms, potential fields, wavelet, kernel poisson, Italy

INTRODUCTION

Recognition of the causative sources of potential field is a long-standing topic and a number of techniques have been proposed to solve the problem. These techniques generally consist of two categories: processing and inversion. The latter one concerns the methods for which the main goal is to recover the source distribution responsible from the measured potential field while the former one transfers the field data into a auxiliary spaces such as the Fourier domain, reduction to the pole, upward continuation, horizontal derivatives, vertical derivatives and wavelet transform from which the source parameters are easier to obtain.

In this study we follow the processing approach and transfer the potential field data into the wavelet domain space. The wavelet transform has several advantages with respect to the other methods. It represents a local analysis (time, space) of the measured field. This transform also removes the high frequency noises as it acts as an upward continuation operator (Baranov, 1957; Blakely, 1995).

Wavelet transform: There are numerous methods to signal processing. Most well-known of these methods is Fourier analysis. This analysis transfers the signal form time domain to frequency domain. In the frequency domain only the frequency characteristics of signals are existed and time characteristics are vanished. It means we cannot determine the time of a frequency event. Denis Gabor utilized Furrier transform for equal and small parts of signal to solve this problem. This technique (windowing signal) called short time furrier transform. Using a window with constant size all signal frequencies is not detectable. To recognize low and high frequencies, large and small windows are used, respectively. Thus,

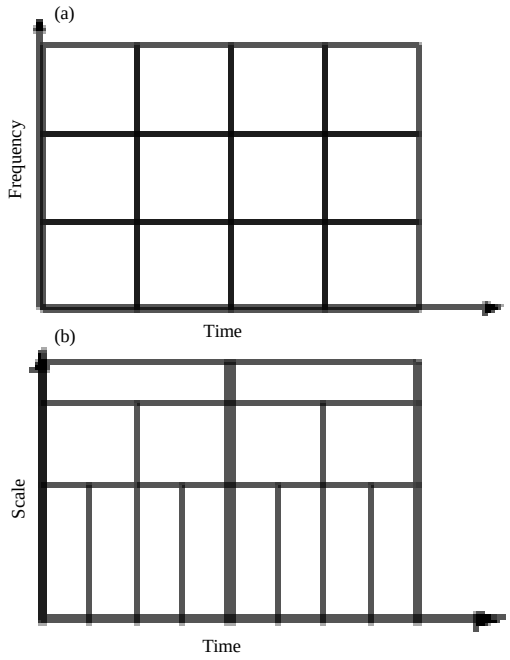

Fig. 1: a) Short time Fourier transform and b) wavelet transform for different scales of wavelet

some information on frequency is lost in order to determine the time of event. Wavelet transform is a window technique which utilizes the method of changing size of a window. Figure 1 shows the difference between short time Fourier transform and wavelet transform. In summary, this transform computes the correlation of various parts of a signal with analyzing wavelet. The amounts of correlation are called wavelet coefficients. Wavelet coefficients are computed for different scales of wavelet. Wavelet scale has a reverse relation with

Corresponding Author: Arash Amirian, Faculty of science, Razi University, Kermanshah, Iran

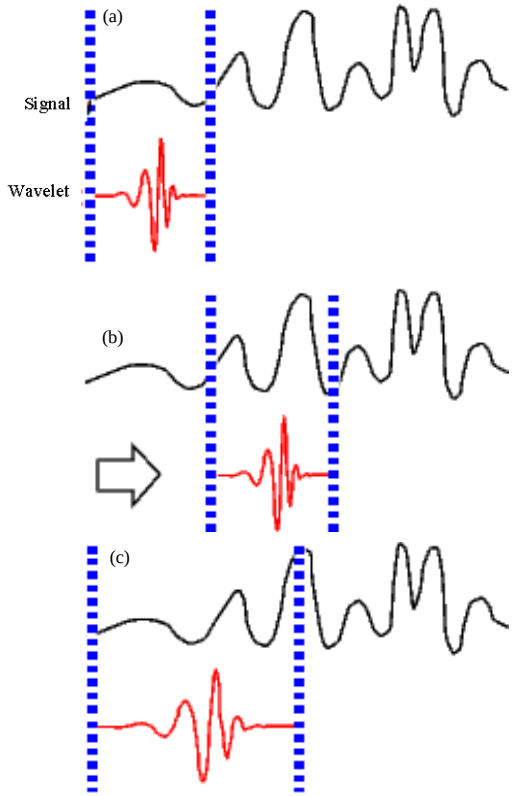

Fig. 2: Wavelet coefficients at various times and scales: a) determining wavelet correlation with all parts of the signal; b) wavelet displacement along the signal until covering whole of the signal and c) iterating the steps a and b with different scales

frequency. Then, the high scales show properties of a signal in low frequency and vice versa. For obtaining wavelet space of a signal, following steps should be considered (Gibert *et al*., 1997):

- Computing the correlation of wavelet with a part of the signal
- Displacing the wavelet along the signal and computing correlation through all parts of the signal
- Iterating steps a and b for different window sizes (various scales of wavelet)

Figure 2 shows the different parts of wavelet transform. Finally, wavelet transform consists of coefficients at various times and scales. Function $\Psi(t)$ can be considered as a wavelet if and only if:

$$c_\Psi = \int_0^\infty |\Psi(\omega)|^2 \frac{d\omega}{|\omega|} < \infty \quad (1)$$

The only constrain is:

$$\int_{-\infty}^{+\infty} \Psi(t)dx = 0 \quad (2)$$

$\Psi(\omega)$ is Fourier transform of $\Psi(t)$.

MATERIALS AND METHODS

Wavelet transform of potential fields: Let s and g are considered to be complex valued functions over R^n space. Wavelet transform of s with respect to analyzing wavelet g is defined as (Moreau *et al*., 1999):

$$w[g, s] \equiv \int_{R^n} dx \frac{1}{a^n} \bar{g}\left(\frac{x-b}{a}\right) s(x) \quad (3)$$

$$w[g, s] \equiv \int_{R^n} dx \frac{1}{a^n} \tilde{g}\left(\frac{b-x}{a}\right) s(x) \quad (4)$$

where, $\tilde{g}(x) = \bar{g}(x)$ and $\tilde{g}(x)$ and is the conjugate complex function of g. The first formula expresses wavelet transform in terms of a correlation function whereas second one is a convolution. Dilation (D_a) is defined as:

$$D_a s(x) = a^{-n} s\left(\frac{x}{a}\right) \quad (5)$$

Then, the wavelet transform can be written in terms of convolution as:

$$W[g, s](b, a) = (D_a \tilde{g} \times s)(b) \quad (6)$$

For a signal of s(x) degree:

$$s(\lambda x) = \lambda^\alpha \quad (7)$$

And:

$$w[g, s](\lambda b, \lambda a) = \lambda^\alpha w[g, s](b, a) \quad (8)$$

S(x) is considered as acquired signal on a profile such that: Ø (x, z = 0) = s(x). The function Ø(x, z) is obtained from Eq. 9:

$$\varnothing(x,z) = w[p,s](x,z) \quad (9)$$

P is Poisson's kernel and is defined as:

$$p(x) = c_{n+1}(1 + |x|^2)^{\frac{-(n+1)}{2}} \quad (10)$$

n denotes physical dimension. In two dimensional physical spaces, n equals 1. If field Ø is transferred

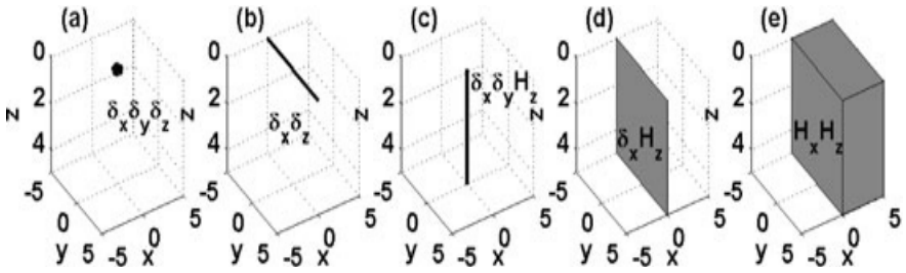

Fig. 3: Schematic diagram of simple homogenous sources: a) point source (a = –3); b) infinite horizontal line; c) infinite vertical line; d) infinite thin vertical sheet and e) contact (Sailhac *et al*., 2009)

to a wavelet space by Poisson wavelets, the following relation is verified (Moreau *et al*., 1999):

$$W[g, \varnothing(0, z)](b, a) = \left(\frac{a}{a''}\right)^{\gamma}\left(\frac{a'' + z}{a + z}\right)^{\gamma+n-\alpha-2} W[g, \varnothing(0, z)]\left(b\frac{a'' + z}{a + z}, a''\right) \quad (11)$$

g is a wavelet in above relation Eq. 11 which is in place of Poisson kernel in relating Eq. 7 and is obtained from derivative of Poisson kernel. γ is the degree of derivative (wavelet homogenous degree) and α is the degree of field or source homogeneity. Equation 9 states that the points (b, a) and:

$$\left(b\frac{a'' + z}{a + z}, a''\right)$$

have the same phase in wavelet space. In other words, if (b, a) becomes maximum, point:

$$\left(b\frac{a'' + z}{a + z}, a''\right)$$

is maximum, too. It is convenient to show if lines that cross at these two purposed points in wavelet space (extreme lines), they cross at point (0, -z). The equation of this line is:

$$y = \frac{a + z}{b} - z \quad (12)$$

(0, -z) is the center of homogenous source potential or the place of homogenous source. For all potential sources, this point always gives the upper edge of source except in case of sphere. In the latter case, the point is sphere center because sphere center is its homogenous center. For an infinite vertical line, homogenous center is the upper edge of it. This method is able to determine depth of any potential source with good precision. Wavelet coefficients variations at extreme points in wavelet space relates with source homogeneity degree as (Gibert and Moreau, 2000; Gibert and Passel, 2001):

$$\mathrm{Log}\left(w_{\alpha}/\alpha^{\gamma}\right) = \beta\log(a + z) + \mathrm{cte} \quad (13)$$

β is slope of above equation and z is depth. The relation of β for magnetic field is $\beta = \alpha$-γ while for gravity field is $\beta = \alpha$-γ-1 (Sailhac *et al*., 2009). This difference comes from the fact that structural index for a magnetic shape is greater than for a gravity shape by 1 (Bleakly, 1995). α is homogeneity degree in these relations. Therefore, we have found a solution for homogenous degree of a source from which an estimation of source shape may be obtained. It is emphasized that source should be homogenous.

Degree of homogeneity for point source α = -3, infinite horizontal line α = -2, infinite vertical line α = -1, infinite thin vertical sheet α = -2 and contact α = 0 (Sailhac *et al*., 2009) (Fig. 3).

RESULTS AND DISCUSSION

Infinite magnetic horizontal line: We consider an Infinite magnetic horizontal line at depth z = 50 m which is magnetized uniformly. Magnetic response of this model is shown in Fig. 4.

For wavelet transform of signal above, 3th order wavelet (γ = 3) is used. Wavelet transform coefficients related to 3 scales, 10, 30 and 50 are shown in Fig. 5.

In Fig. 5, it is seen that relative extremes around x = 500 m have amplitudes greater than those points far away from it. In Fig. 6, relative extreme points have been drawn to scale equals 80. Red points are related to maximum points while blue ones are minimal.

Wavelet space extremes around the source are placed on lines which converge toward the source while far away the source maximums and minimums are placed on each other. One constraints for converging of extreme lines relative to the source position is source homogeneity ($s(\lambda r) \neq \lambda^{n} s(r)$). For homogeneity of source two conditions should be satisfied: homogeneity of properties of the source (magnetization, density or conductance) and relation between amplitude of the field to distance from source such that: $\Phi(\lambda r) \neq \lambda^{\alpha} \Phi(r)$. In very low scales, homogeneity condition is failed because field amplitude

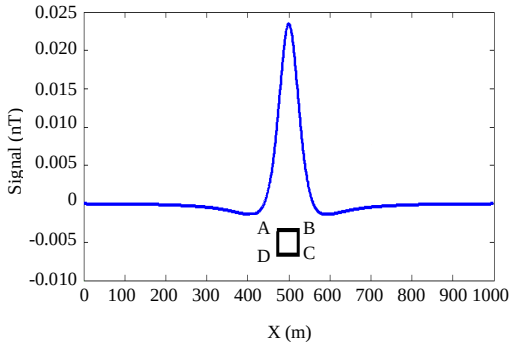

Fig. 4: Magnetic response of an infinite magnetic horizontal line

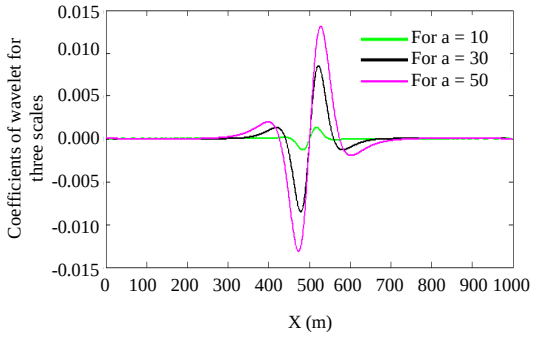

Fig. 5: Wavelet transform coefficients of the signal resulted from infinite horizontal line at three different scale

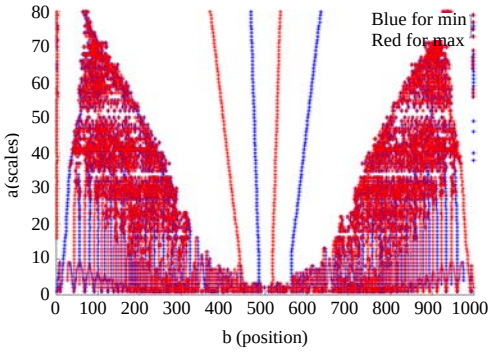

Fig. 6: Wavelet space extremes at points far away the source coincides with each other and they do not converge. At lower scales, there also exists a little deviation

is not depended only on the distance. Consequently, extreme lines have a little deviation. Thus, only higher scales are considered. In Fig. 7, only extremes around the source with scales greater than 10 have been mapped

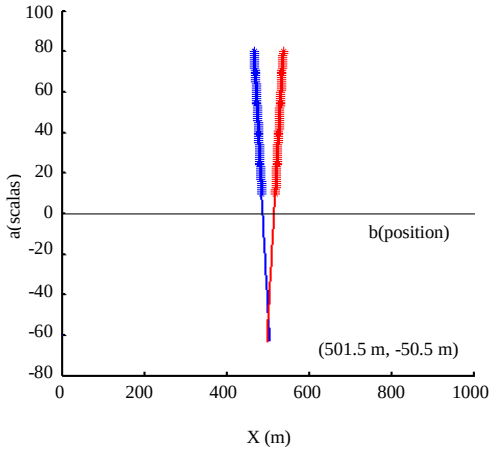

Fig. 7: Absolute extremes for scales >10 are drawn. The lines are convergent at the source position

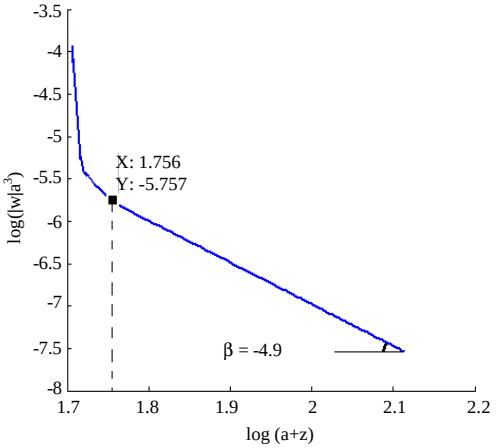

Fig. 8: Determination of homogeneity degree

and the extreme lines converge at points x = 501.5 and z = 50.5 m) (Boukerbout *et al*., 2003; Hornby *et al*., 1999).

Variations of log (w/α^{γ}) in terms of log (α+z) is shown in Fig. 8. According to Fig. 8 as $\gamma = 3$ and $\beta = -4.9$, using relation $\beta = \alpha - \gamma$, the degree of homogeneity is equal to -1.9 which is for an infinite horizontal line as we have purposed. Variation of slope of the line in Fig. 8 is due to the effect of low scales which occurs at scale 8.

Dyke model (gravity example): A dyke is considered with these characteristics: width = 200 m, upper depth = 30 m and density = 2.5 g cc^{-1}. Edges of this model are at 400 and 600 m. Wavelet space extremes of gravity field wavelet transform is shown in Fig. 9. Extreme lines are seen near the edges and the flanks. Latter ones converge and have weak amplitude and are not related to position of the

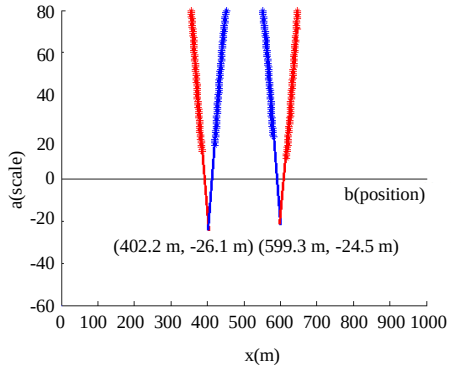

Fig. 9: Extreme lines of a dyke

source. The former ones converge which point to edges and depth of the model x = 402.2 m, z = 26.1 m and x = 599.3 m, z = 24.5 m (Fig. 9).

Effect of noise: Consider a signal with noise defined as:

$$d(x) = \varnothing_0(x) + v(x) \tag{14}$$

V(x) indicates noise and Ø0(x) gives the signal caused by the source. Conducting wavelet transform:

$$w[g, d](b, a) = w[g, \varnothing_0](b, a) + w[g, v](b, a) \tag{15}$$

Equation 15 shows that the signal wavelet transform consists of a definite part W[g, Ø0](b, a) and a probable part W[g, v] (b, a). It is noticeable that probable part is dependent on statistical characteristic of noise.

If v(x) is Gaussian noise with the mean of zero value and variance of 10^{-6}, linearity of wavelet transform ensures us that W[g, v](b, a) is Gaussian with variance defined as (Moreau *et al*., 1999):

$$\sigma_v^2 \int_{-\infty}^{+\infty} (D_a g)^2(x)dx = a^{-n/2}\sigma_v^2 \int_{-\infty}^{+\infty} g^2(\varepsilon)d\varepsilon = a^{-n/2}\sigma_v^2 E_g \tag{16}$$

In which:

$$E_g = \int_{-\infty}^{+\infty} g^2(\varepsilon)d\varepsilon$$

is wavelet energy. Equation 16 shows that the variance of wavelet transform of W[g, v](b, a) is $a^{-n/2}$ which changes with scale. Consequently, wavelet transform is more affected in low scales than high ones. We expect that from a threshold scale, noise effect is significant and vice versa:

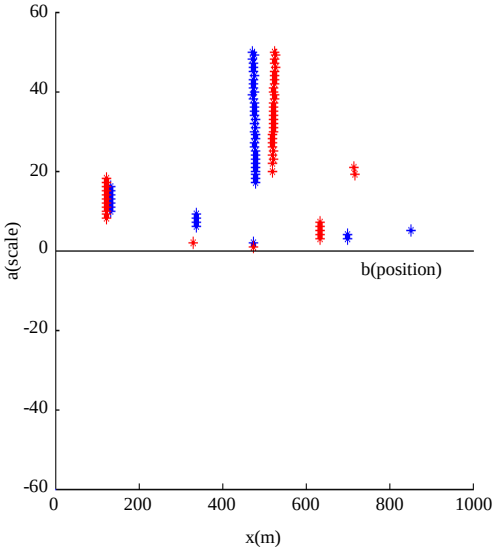

Fig. 10: Absolute extreme points from a = 1-50

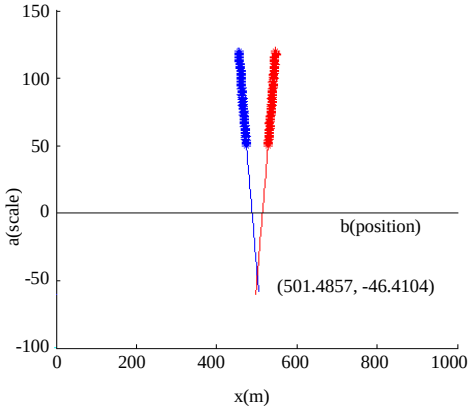

Fig. 11: Absolute extreme points for a = 50-120

$$w[g, d](b, a << a_c) \approx w[g, v](b, a) \tag{17}$$

According to definition a_c is correspondent to a scale in which ratio of signal to noise is from order 1. We add Gaussian noise with mean of 0.05 and variance 5×10^{-6} nT to the signal caused by infinite horizontal line. Noisy signal is shown in Fig. 10 (Telford *et al*., 1976).

Plotting wavelet transform extremes in low scales and at presence of noise has no clear result. In these scales, noise amplitude is proportional to amplitude of the signal and extreme lines are far from position of the source.

Figure 10 shows, for scales smaller than a_c = 20, relative extremes are not close to the source x = 500 m. However, extremes mostly which are caused by noise are at farthest points of the source. We have plotted extremes for scales of 50-120 (Fig. 11). For these scales, all extremes

Fig. 12: Albuquerque Basin inside Rio Grande and San Ysidro fault (Grauch *et al*., 2006)

are close to the source, because noise effects have been reduced and the convergence point is at (501.4, -46.4 m).

To test the validity and accuracy of methodology, we conducted the continuous wavelet transform to interpret aeromagnetic data of San Ysidro fault of Rio Grande Rift in USA. The fault was studied in Grauch *et al*. (2006). This fault has a NNE-SSW striking and is a normal fault in Albuquerque sedimentary basin (Hsu *et al*., 1996; Woodward and Reutschilling, 1976). San Ysidro fault is exposed mainly to the surface (Roy, 2013). Majority of the aeromagnetic data is produced by Santa Fe group of sediments (Grauch *et al*., 2006; Hudson *et al*., 1998). Figure 12 shows the location of Albuquerque Basin inside Rio Grande Rift and general site of San Ysidro fault.

Total Magnetic Intensity (TMI) is gathered on 10 profiles. Every profile is 1650 m long. Distance interval is 50 m. In prior studies, the fault has been detected on profiles. Therefore, we regard their results to evaluate ability of wavelet transform to detect San Ysidro fault. It is worth mentioning that continuous wavelet transform have not been employed to detect faults.

Figure 13a shows total magnetic intensity on profile A. According to the figure, changes of TMI are not smooth. Figure 13b also illustrates wavelet transform of TMI. In Fig. 13a, b is the vertical axis showing the scale.

Also, b is the horizontal axis showing the number of data on the profile. Depth and horizontal location of the fault are calculated by multiplying 50 (distance interval) in the values of a and b of convergence point, respectively. Since, we multiply 50 in the values of a and b, therefore, small change in the value of a and b may lead to a large changes in results.

Figure 13b, the amounts of a and b are -10 and 700, respectively. This means the depth of fault is 500 and horizontal location of fault is at 850 m. According to Jemezpprofs's survey, depth of the fault is 50 m and its

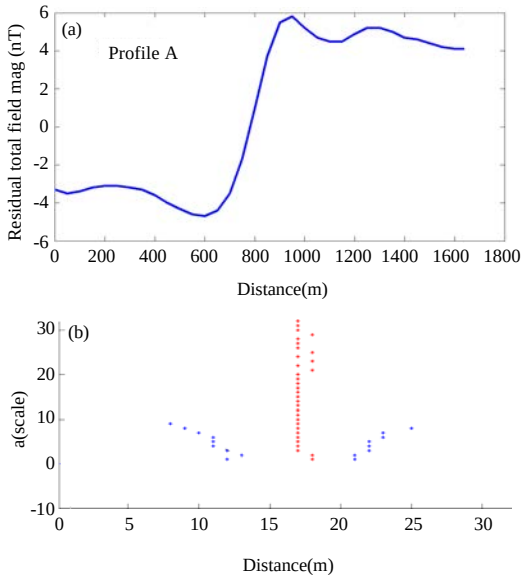

Fig. 13: a) TMI measured on the profile and b) wavelet transform of TMI shows the location of the fault

horizontal location is at 700 m. This difference is due to the distance interval. It is rational that distance interval is an important factor to approximate also the depth of fault. The results of wavelet transform are affected by noise. Thus, to improve results we conduct upward continuation filter on data to reduce effects of noise.

The data set is filtered by upward continuation to a specific level to obtain a Fig. 14a. After upward continuation, the number of output data was more than the number of input data and distance interval decreased to 12.6 m. Thus, upward continuation has two advantages. First, it reduces noise effects and improves final results. Second, distance interval decreases. So, error in depth approximation decreases from 50-12.6 m. Figure 14b, shows coefficients of wavelet transform after upward continuation. In this situation the coefficients of wavelet transform are more precise. However, they are not linear like coefficients of synthetic models. Linearity state in only pertained to the isotropic magnetic source. In this state, to find convergence point, curves should be extended. We carried this out by inserting black points in 14 b. The amounts of a and b are -5 and 65, respectively. These values indicate that the depth is 63 m and horizontal location is at 820 m. These results are close to the results of Jemezpprofs's survey (Hudson *et al*., 1998; Kearey *et al*., 2002).

In next step, by averaging the output of upward continuation filter, distance interval was decreased from 12.6-6.3 to reduce error of calculated a and b. in this state, the diagram of signal is similar to 14a, only number of data is doubled. Figure 14c is diagram of coefficients of wavelet transform. According to Fig. 14c, values of a and

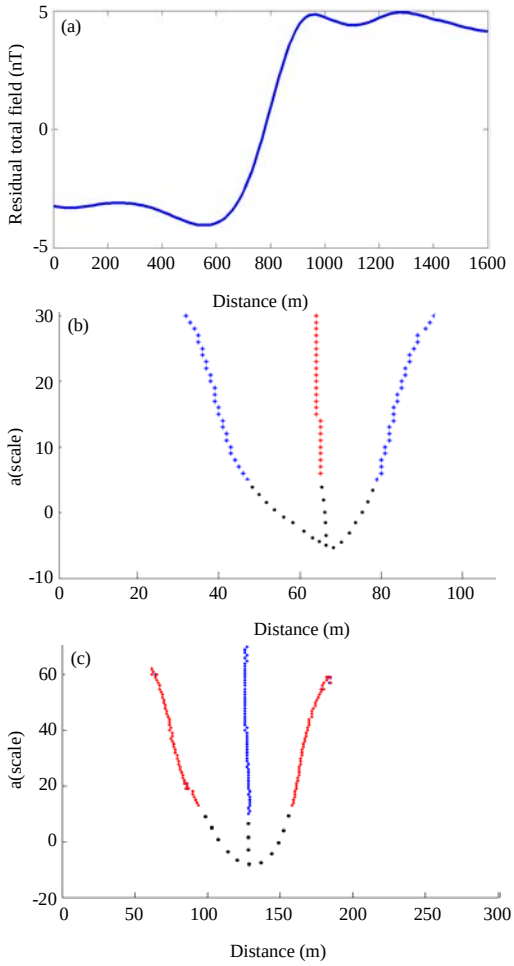

Fig. 14: a) TMI continued to a surface above ground; b) wavelet transform of continued data determines location of the fault precisely and c) wavelet transform of the average of continued data yields more precisely the location of the fault

b are -10 and 125, respectively. These amounts are corresponding to 63 and 790 m for depth and horizontal location, respectively.

CONCLUSION

In this research we employed wavelet transform to detect two synthetic models and San Ysidro fault in USA. Wavelet spaces pertaining to these sources yield the values of depth and horizontal location of targets. Results of wavelet transform are more exact in homogenous ambiences. Method utilized in this research, approximated edge of synthetic models as well depth and horizontal location of the San Ysidro fault. To reduce error in field example, upward continuation filter was conducted.

REFERENCES

Baranov, V., 1957. A new method for interpretation of aeromagnetic maps: Pseudo-gravimetric anomalies. Geophys., 22: 359-382.

Blakely, R.J., 1995. Potential Theory in Gravity and Magnetic Applications. Cambridge University Press, Cambridge.

Boukerbout, H., D. Gibert and P. Sailhac, 2003. Identification of sources of potential fields with the continuous wavelet transform: Application to VLF data. Geophys. Res. Lett., 30: 1-4.

Gibert, D. and F. Moreau, 2000. Identification of sources of potential fields with the continuous wavelet transform complex wavelets and application to aeromagnetic profiles in French Guiana. J. Geophys. Res., 105: 19455-19475.

Gibert, D. and M. Pessel, 2001. Identification of sources of potential fields with the continuous wavelet transform: Application to self-potential profiles. Geophys. Res. Lett., 28: 1863-1866.

Gibert, D., M. Holschneider and G. Saracco, 1997. Wavelet analysis of potential fields. Inverse Prob., 13: 165-178.

Grauch, V.J.S., M.R. Hudson, S.A. Minor and J.S. Caine, 2006. Sources of along-strike variation in magnetic anomalies related to intrasedimentary faults: A case study from the Rio Grande Rift, USA. Explor. Geophys., 37: 372-378.

Hornby, P., F. Boschetti and F.G. Horowitz, 1999. Analysis of potential field data in the wavelet domain. Geophys. J. Int., 137: 175-196.

Hsu, S.K., J.C. Sibuet and C.T. Shyu, 1996. High-resolution detection of geologic boundaries from potential-field anomalies: An enhanced analytic signal technique. Geophys., 61: 373-386.

Hudson, M.R., M. Mikolas, J.W. Geissman and B.D. Allen, 1998. Magnetic properties of Santa Fe Group sediments in the 98th Street core hole, Albuquerque, New Mexico. New Mexico Office of the State Engineer, Albuquerque, New Mexico.

Kearey, P., M. Brooks and I. Hill, 2002. An Introduction to Geophysical Exploration. Wiley-Blackwell, Hoboken, New Jersey, USA.,.

Moreau, F., D. Gibert, M. Holschneider and G. Saracco, 1999. Identification of sources of potential fields with the continuous wavelet transform: Basic theory. J. Geophys. Res. Solid Earth, 104: 5003-5013.

Roy, I.G., 2013. Tilt angle interpretation of dipping fault model. J. Appl. Geophys., 98: 33-43.

Sailhac, P., D. Gibert and H. Boukerbout, 2009. The theory of the continuous wavelet transform in the interpretation of potential fields: A review. Geophys. Prospect., 57: 517-525.

Telford, W.M., L.P. Geldart, R.E. Sherief and D.A. Keys, 1976. Applied Geophysics. Cambridge University Press, Cambridge.

Woodward, L.A. and R.L. Reutschilling, 1976. Geology of San Ysidro Quadrangle. New Mexico Bureau of Geology and Mineral Resources, New Mexico, USA.